A COMPACT FRACTAL ANTENNA FOR 5G MODERN VEHICULAR APPLICATION

N. Porchelvi[1], S. Nithya[2], A. Sandhiya[3], S. Shiva Shalini[4], C. Yogeshwari[5]

[1] N. Porchelvi. Assistant Professor, Department of Electronics And Communication Engineering, Vivekanandha College of Technology for Women, Tamil Nadu, India.

[2,3,4,5] Students, Department of Electronics And Communication Engineering, Vivekanandha College of Technology for Women, Tamil Nadu, India.

Abstract:

This study presents and integrates a new fractal iterative structure of a progressive defect patch with a triangular array structure. To achieve broadband operations, the antenna patch is designed using fractal geometry and a rectangular slot for feed. The antenna archives return losses of less than –10dB. The proposed antenna achieved a total gain in the operating band with a highly directive and efficient range of operation. Results from simulations and measurements are contrasted and found to be accord.

Keywords: *Fractal Geometry, Recessed Ground, 5G, millimeter communication, Vehicular Communication Applications.*

1. Introduction:

In the present generation, there is a huge demand for connected vehicles and the features evolved using high-frequency communication. The automotive industry has had a significant impact from vehicular communication thanks to its top-notch safety and security capabilities. The communication is mostly referred to as Vehicle to Everything(V2X) communication which involves many standards such as pedestrian, infrastructure, cloud, fog, driver, and other nearby vehicles. [1] An ultra-wideband antenna is constantly in great demand to provide all these qualities. Throughout the decades, designers have developed a wide range of antenna designs to meet current demands for 4G communication frequencies. Future connected vehicles will be constrained bythe current 4G cellular systems and the Dedicated Short- Range Communications (DSRC) spectrum allotted for vehicular communications. Most designs make use of the available frequency spectrum up to 6GHz. connected vehicles will be constrained by the current 4G cellular systems and Dedicated Short-Range Communications (DSRC) spectrum allotted for vehicular communications. Most designs make use of the available frequency spectrum up to 6GHz. connected vehicles will be constrained by the current 4G cellular systems and Dedicated Short-Range Communications (DSRC) spectrum allotted for vehicular communications. Most designs make use of the available frequency spectrum up

to 6GHz. A lot of interference is observed when these frequencies are used for communication. [5] A new set of frequencies needed to be established to communicate without interference. The most appropriate method is to shift the gear from 4G to 5G which is designed for enabling instantaneous connectivity to billions of devices across the human earth which leads to a truly connected universe with speeds that are ten times better than that of the previous generation. Low latency and stable connectivity will enable a new generation of applications in almost all domains. Even fantasies have bounds, but 5G will have no such restrictions in terms of services and economic potential. [1]

1.1 Similar works:

The most recent research initiatives in the areas of fractal antennas, 5G communications, and vehicular communications are presented in this section. [14] The focus is on the properties of the antenna and its behavior at future frequencies. The authors suggested a hexagonal-shaped ultra- wide bandwidth Fractal dipole antenna with a frequency range of 0.5–12 GHz. [5] The simulation was done with a focus on the antenna's gain, which for various penetration angles averaged 6.9 dBi. The previously presented fractal module is incredibly compact and can be used for vehicle communications. With a minimum reflection coefficient of 29.18 dB, the VSWR was in the range of 3.4 dB. In the analysis that followed, the author proposed a triangular-shaped fractal geometry antenna for usage in UWB applications. The self-complementing idea is applied to the first iteration of the planner triangular monopole antenna enhancement. It is observed that this strategy reduces the reflection coefficient to below 10 dB for the frequency range of 4-10 GHz. When compared to single and multiple patches, the triangle patch's performance level was up to 30% better. [7] We develop single-layer patch antennas as well as multi-layer antennas intending to analyze this antenna. The antenna's ability to be employed in a variety of applications is one of its primary qualities. For extremely wide-band applications, the author proposed a hexagonal wide slot antenna based on fractals. At frequencies between 3 and 30 GHz, the suggested antenna achieves a ratio impedance bandwidth of 15:19 for a VSWR of 1. When compared to the bandwidth needed for SWB functioning, the realized bandwidth is twice as large. [2]

The author suggested a hexagonal tuning stub loaded at the microstrip feed line for bandwidth increase, even at lower frequencies, which is a great concept for the small antennas that can be mounted on a vehicle. The antenna must now be wearable and conformal so that it may be positioned on a person's body and deliver the necessary data [13]. For improved antenna performance and SAR reduction, the author suggested a wearable Fractal monopole antenna incorporated with a reflector. At an operating frequency of 2.36–2.50 GHz, the suggested antenna exhibits enhanced bandwidth of 130 MHz in free space and 128 MHz when placed on a at homogenous phantom. The most crucial component of any antenna, according to 484 A. RAHIM ET AL., is its bandwidth [21]. For UWB applications, the author

proposed a fractal antenna with a modified hexagonal form with multi-band notch characteristics. FR4 Epoxy was used to manufacture the antenna, resulting in a bandwidth of 2.36 GHz in the frequency range of 9.6 GHz–15 GHz and an S11 of less than 10 dB across the full UWB range. The author noted that these enhanced qualities have several uses in the telecommunications and vehicular communications-industries.

Our knowledge of how to construct the suggested work has significantly improved as a result of the research indicated above, making it more applicable to multi-band applications in vehicular communications in 5G scenarios. To obtain broadband and multi-band characteristics with wide impedance, slots have been added to the design.

2. Introduction to fractal structure of gradual defect patch:

The term "fractal," which is used to deny a class of geometric structures with self-similar features, was initially put out by French mathematician Mandelbrot in 1983 [24]. The fractal theory is now being used more and more in antenna design. The fractal structure's self-similarity causes the current distribution inside the antenna to be relatively uniform, its working bandwidth to be higher, and its intricate folding structure to enable the antenna to be made smaller. The progressive defect patch fractal structure and its fractal iteration process are both new structures. A triangle that has been further divided serves as the basic building block of the progressive defect patch's fractal structure. The array element antenna in the design of the antenna structure is the gradual defect patch fractal antenna. The progressive defect patch fractal is self-similar in both its entirety and its parts. Within the fractal structure, the radiofrequency current can be dispersed very equally [8]. The antenna is quite good. When the radiating antenna patch is designed using the fractal structure of the gradual defect patch, broadband working performance is achieved. The progressive defect patch fractal includes numerous defects with various side lengths that act as "digging holes," creating numerous radiation slits of various lengths that operate in various frequency bands, and their radiation superposition can create a wider operating bandwidth [9].

2.1 Design methodology:

The following flow diagram symbolizes the workflow in designing conventional patch antennas in HFSS.

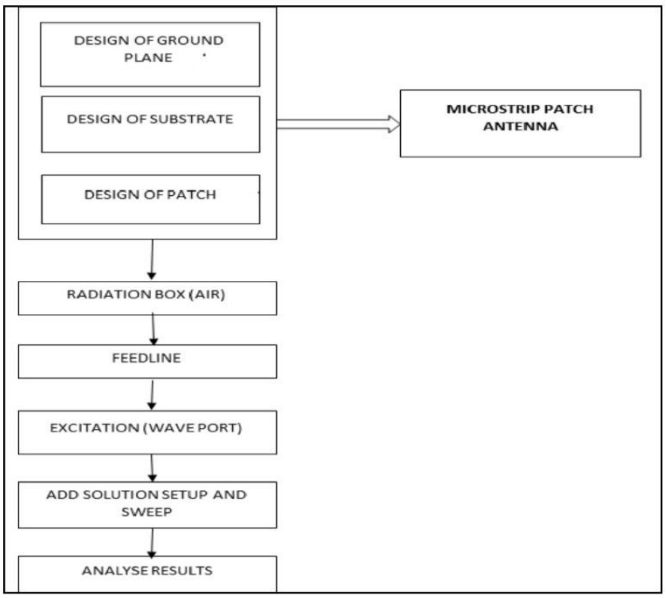

The antenna was initially designed using Ansys EM (HFSS) software. It is fed by a slot line, on which an SMA connector is soldered for measurements [17]. The

design is indicated and inspired by the need for the antenna to resonate in two different frequencies [14]. The resonator close to C-V2X frequency bands and the extended half circles allow the antenna to operate at the lower cellular frequencies.

2.2 Proposed Antenna Geometry:

In this section, the designing procedure of the proposed fractal antenna with defected ground has been described in detail along with the substrate material and its properties are described.

object	values
L1	20mm
L2	23mm
L3	16mm
Substrate thickness	1.6mm
Outer triangle	20mm
Inner triangle	16mm
Substrate dimension	41.7mm× 41.7mm
Substrate used	FR4 Epoxy
Substrate permitivity	4.4

Table 1: Parameters of Proposed Antenna

Material name	Relative permittivity (εr)	Mass density (kg/m3)	Dielectric loss tangent
FR4	4.4	1900	0.02
Rogers-RT/duroid 5880 (tm)	2.2	0	0.0009
Arlon AD45((tm)	4.5	0	0.0035
Bakelite	4.8	1300	0.002
Glass	5.5	2500	0
Polyester	3.2	0	0.003

Table 2. Parameters of different substrates materials.

The antenna is designed and simulated using HFSS and obtained a good output response. It resonates at frequency ranges of 4.7, 5.9 GHz, which makes it suitable for 5G applications [4].

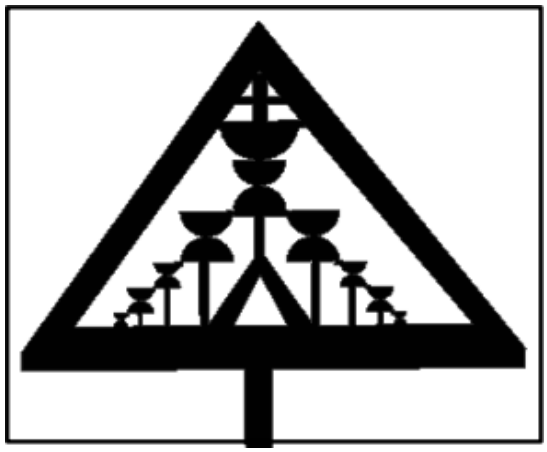

Fig 1. Top view of the proposed antenna

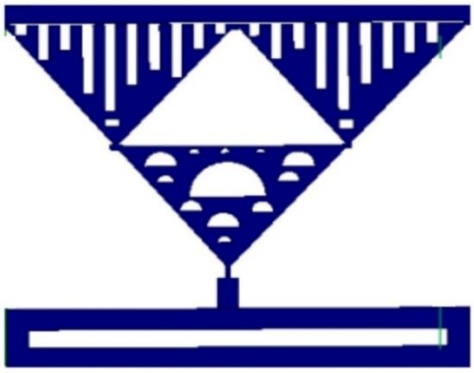

Fig 2. Bottom view of the proposed antenna

2.3 Antenna Design and Simulation Results:

The antenna's radiation pattern is distorted at the higher frequency bands. The antenna at 5.9 GHz is not designed to be linearly polarized due to the SMA (Sub-Miniature version A) connector, the size of the feedline is comparable to the wavelength since the cross-polarization is created due to the transverse currents of the higher order modes [13]. The co- and cross-polarization of the antenna as simulated in Ansys EM (HFSS) and measured during the various experimental setups are indicated. The measured maximum values of the co polarization are higher than the simulated one.

The reflections created by the obstacles in the real environment, the ground, and the vehicle's body modify the antenna's radiation patterns and add more to its maximum radiation pattern values [15]. The smallest value of the cross-polarization at the angle where we have the maximum co-polarization value at 5.9 GHz when the vehicle is present, is measured to be −10 dBi when the antenna is placed inside themirror's cover [3].

Fabricated antenna:

The following diagram shows that the fabricated antenna of proposed geometry.

Fig.3 Top view of antenna

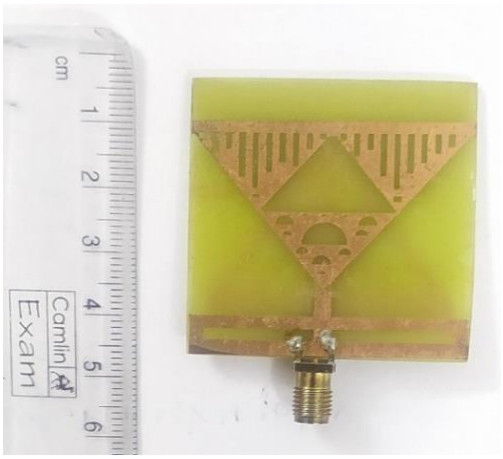

Fig.4 Bottom view of the antenna

The proposed geometry of the antenna system is better at maintaining the total conductivity and radiating characteristics of the antenna. The antenna is 59 mm in totaland the length of the three sides are 20, 23, and 16 mm, while the height of the substrate is 1.6 mm, loss tangent, tan δ = 0.019, and dielectric constant εr = 4.4. For the second iteration, the fractal antenna had made a further small triangle slot at its center. Furthermore, the miniaturization produced seven smaller half-circles inside of a large triangle in the third iteration. The smaller compact half circles within the patch increase the surface radial current distribution and, hence, the overall conductivity of the patch's energy, resulting in stronger radiation.

2.4 Performance Evaluation:

Simulated and measured results of the proposed compact fractal antenna in terms of performance parameters like reflection coefficient, VSWR, gain, current distribution, and radiation pattern are discussed in this section. Also, the effect of different parameters like the height of the substrate, size of the ground plane, substrate material, and feed width is studied.

2.5 S11 Parameter and VSWR:

The S11 parameter denies the extent of backscattering thatoccurred at the required frequency [26]. The return loss or reflection coefficient or S11 is the fundamental parameter to observe the radiation efficiency of an antenna. It gives information about the extent of the electromagnetic wave reflected toward the tested antenna. The reflection coefficient versus frequency plot

for the 0th, 1st, and 2nd iterations of the proposed antenna are shown in Fig. 5. The 2nd iteration shows more bandwidth as compared to the 0th and the 1st iterations.

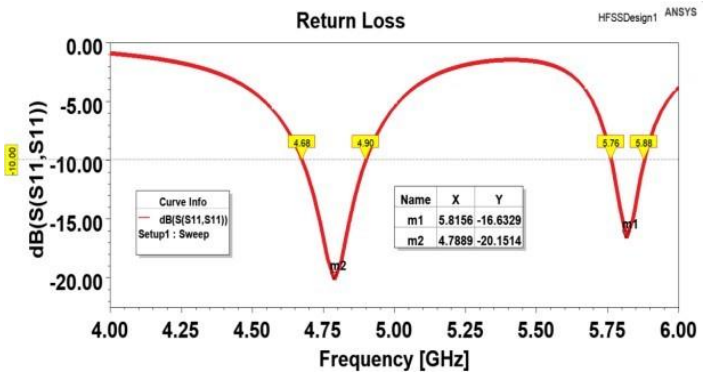

Fig. 5: S11 versus frequency plot for different iterations.

The simulated and measured S11 versus frequency plot and VSWR versus frequency plot for CFA are shown in Fig. 5 and 6 respectively. The value of VSWR lies between 1 and 2 at all resonant frequencies which are 1.21 and 1.34 showing that the proposed antenna source and load terminal are perfectly matched at these frequencies.

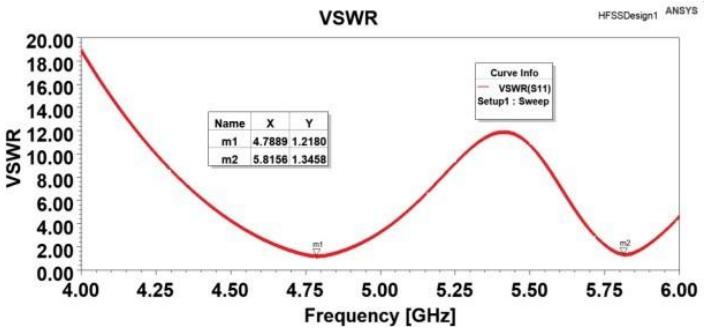

Fig. 6: Comparison of simulated and measured VSWR

2.6 Impedance:

The impedance plot for the CFA in the Smith chart is shownin Fig. 7. Some frequencies lie near 1 (Re=1, Im=1), and at these frequencies, the impedance is highly matched. There are two types of lines in the Smith chart horizontal and vertical. The horizontal line indicates the imaginary value of impedance, and the vertical line indicates the real value of impedance. Impedance is perfectly matched when real and imaginary lines cut each other [22]. This graph shows that the proposed antenna is perfectly matched at different resonant frequencies.

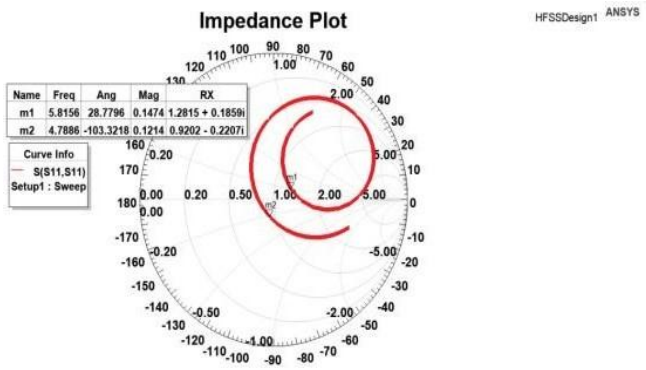

Fig. 7: Impedance plot at smith chart

2.7 Radiation Pattern:

It represents the geographical area at which the antenna can transmit electromagnetic waves surrounding the antenna [8]. There are two major angles azimuth (Eφ) and elevation (Eϕ), which represent the XY plane and YZ plane respectively [12]. The azimuth angle is measured at 0° in thered color line and the elevation angle is measured at 90° in the green line. The radiation patterns at different angles are calculated for 2D far-eld radiation and gain is assigned along with the radiation pattern. The radiation patterns areobserved at phi 0° and 90°, and theta 180° and 270° at everyresonant frequency [19]. The radiation patterns as shown in Fig. 8 represent that the proposed CFA can operate omnidirectionally as well as bi-directionally.

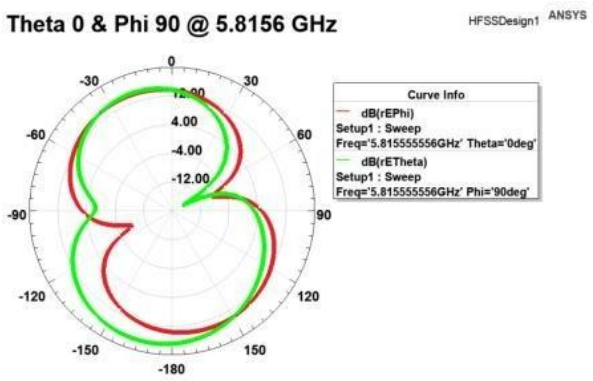

Fig. 8(a)

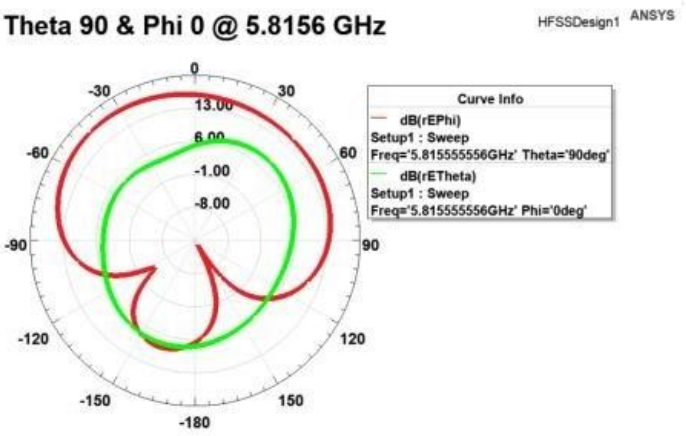

Fig. 8(b)

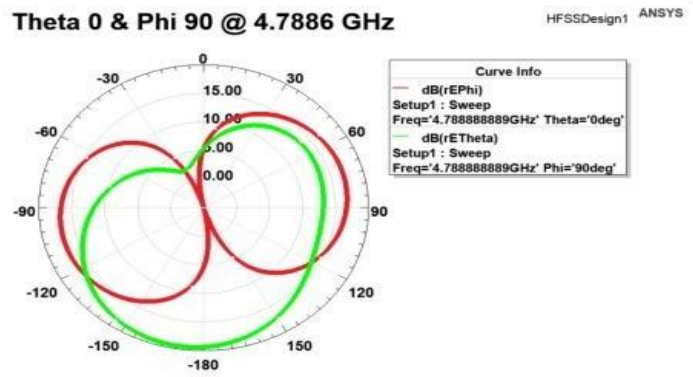

Fig.8(c)

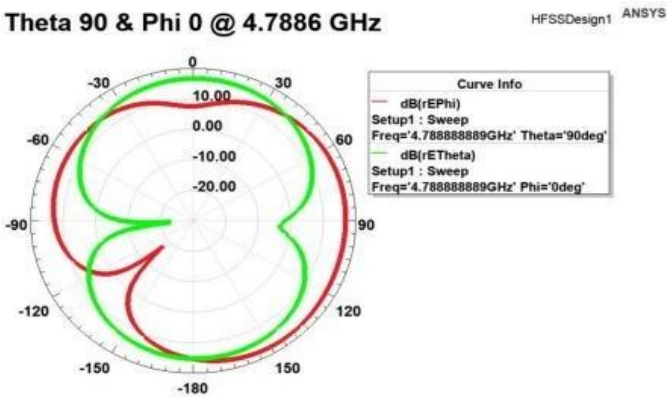

Fig. 8(d)

The gain and directivity of an antenna is calculated at a 3D far field plot at the resonant frequency as shown in Fig. 9(a) & (b).

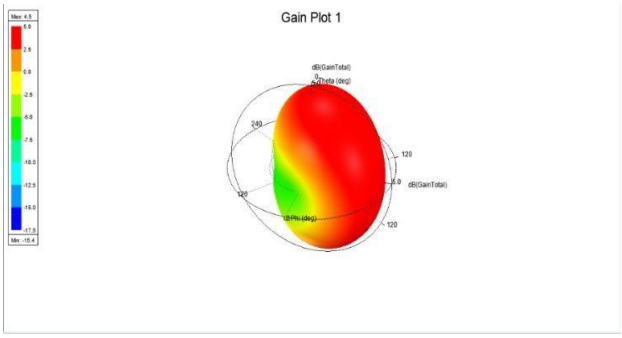

Fig. 9(a)

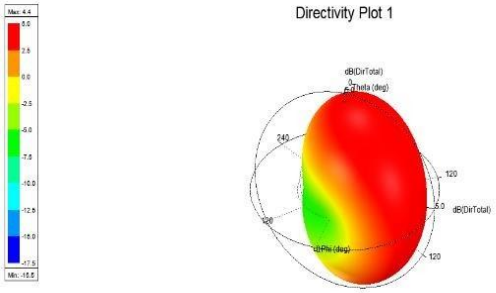

Fig. 9(b)

The electrical magnitudes are strong throughout the antenna and on the patch and ground, which provides excellent stability and radiates the most energy that is taken in at the port.

2.8 Comparing performance parameters:

A comparison of the performance of compact fractal antenna array (CFA) antennas of different iterations with the other conventional GPS navigation antennas is shown in Table 3. One of the advantages of this design is that the radiation pattern in the antenna with a strip is of the broadside type throughout the entire matching bandwidth. Table 3 summarizes the measured gain, axial ratio (AR) bandwidth, and impedance bandwidth of the conventional fractal antenna, with and without defective ground structure, at the mentioned frequencies. The expected improvement in radiation characteristics may be observed clearly, particularly around 3.6 GHz. For correct impedance matching of the fed system with antenna impedance, the CPW-Fed is a one-step system with fed width (f) = 1.6 mm.

Iteration Count	Resonating Frequency (GHz)	Return Loss (dB)	Return Loss Bandwidth (%)	VSWR	Reflection Coefficient
1st Iteration	2.52 5.45	-25 -28	1.58 1.63	1.44 1.0585	−15.3327 −30.92
2nd Iteration	2.6 3.5 5.81	-29 -26 -32	1.26 1.88 1.52	1.1087 1.57 1.1	−25.5933 −13.1 −26.56

Table 3. Comparative analysis of proposed fractal geometry for various iterations.

Ref	Antenna dimension	Substrate used	Operating band (GHz)	Bandwidth (MHz)	Gain in dB
[6]	120 x120 x4.3	FR4 Epoxy	2.4Gh-7.4GHz	750MHz	3dB
[8]	150 x150 x 4	Rogers RT	3.1GHz-10.1GHz	850MHz	6.25 dB
[9]	42 x 33 x 1.58	Electromagnetic bandgap	2.2GHz-2.8GHz	1000 MHz	7.2dB
[11]	64.4 x 53.7 x 3.94	Nonconductive material	2.45GH-5.8GHz	950MHz	5.7dB
[12]	59.9 x 59.9 x 3.7	Textile material	2.45GHz-5.8GHz	1100 MHz	4.2dB
[13]	40 x 40 x 0.503	Teflon	2.45GHz-5.5GHz	950MHz	2.5dB
[14]	32 x 36 x 1.6	Roger/RT 5880tm	3.2GHz-8.8GHz	6060 MHz	5.17 dB
[15]	26 x 30 x 1.53	Polyamide	3.1GHz-10.6GHz	1200 MHz	6.32 dB
Proposed Design	41.X 41.X 1.6	FR4 Epoxy	3.4GHz-5.9GHz	1250MHz	4.5dB

Table 4. Comparison of proposed antenna design with literature.

3. Conclusion:

With this structure, there has been some improvement in return loss and radiation characteristics at lower and higher frequencies. By implementing defected ground structure (DGS), the radiating patch achieves better impedance matching. The simulated radiation characteristics, comprising of return loss, is −25 dB at 2.52 GHz, with a 1.58% return lossbandwidth at the first iteration, where the radiation pattern is directive. The transceiver's simulated return loss was found to be −29

dB at 2.6 GHz and −26 dB at 3.5 GHz, with a 620 MHz bandwidth of −10 dB (1.26%). For the return that has been experimentally confirmed with a return loss of −32 dB at 5.8 GHz, the loss is very promising at 340 MHz bandwidth (1.52%). The findings showed that there was a trade-off between antenna impedance and thickness with bandwidth. In this work, the dimensions of a microstrip patch antenna were reduced using a fractal slot at the ground plane (DGS); gains have been improved substantially by about 4.2 dBi at 2.6 GHz, 3.8 dBi at 3.5 GHz, and 3.6 dBi at 5.8 GHz. It is concluded that in the vertical polarization pattern, the horizontal polarization pattern has the fewest nulls at lower frequencies and more nulls at higher frequencies. Wideband features increase surface current distribution compared to traditional antennas [23]. With the addition of DGS, the size of the second iterated antenna was decreased by 43.67%; additionally, DGS also results in the suppression of higher harmonics. However, DGS reduces an antenna's gain slightly without affecting its efficiency. The difference in gain can be further enhanced by reducing the thickness and varying fractal structures.

References:

1. Peruani, F., Maiti, A., Sadhu, S., Chaté, H., Choudhury, R. R., & Ganguly, N. (2010). Modeling broadcasting using omnidirectional and directional antenna in delay tolerant networks as an epidemic dynamics. IEEE Journal on Selected Areas in Communications, 28(4), 524–531.

2. Navda, V., Subramanian, A. P., Dhanasekaran, K., Timm-Giel, A., & Das, S. (2007). MobiSteer: Using steerable beam directional antenna for vehicular network access. In Proceedings of the 5th international conference on mobile systems, applications and services (pp. 192-205). ACM.

3. Godara, L. C. (1997). Applications of antenna arrays to mobile communications. I. Performance improvement, feasibility, and system considerations. Proceedings of the IEEE, 85(7), 1031–1060. Chakraborty, U., Chatterjee, S., Chowdhury, S. K., & Sarkar, P. P. (2011). A compact microstrip patch antenna for wireless communication. Progress In Electromagnetics Research C, 18, 211–220.

4. Kim, H. B., Hwang, K. C., & Park, Y. B. (2010). Compact stub loaded meander line antenna for wireless USB dongle devices. Microwave and Technology Letters, 52(10), 2279–2282.

5. Cao, H., Hu, Y., & Yang, L. (2021). Towards intelligent virtual resource allocation in UAVs-assisted 5G networks. Computer Networks, 185, article no. 107660. https://doi.org/10.1016/j.comnet.2020.107660.

6. Jeong, M.-W., Ryu, J. Y., Kim, S. H., Lee, W., & Ban, T.-W. (2020). A completely distributed transmission algorithm for mobile device-to-device caching networks. Computers & Electrical Engineering, 87, article no. 106803.
https://doi.org/10.1016/j.compeleceng.2020.106803

7. Kbashi, H. J., Sharma, V., & Sergeyev, S. (2021). Dual-wavelength fiber-laser-based transmission of millimeter waves for 5G-supported radio-over-fiber (RoF) links. Optical Fiber Technology, 65, article no. 102588.
https://doi.org/10.1016/j.yofte.2021.102588

8. Li, L. (2020). Real time auxiliary data mining method for wireless communication mechanism optimization based on internet of things system. Computer Communications, 160, 333–341. https://doi.
Org/10.1016/j.comcom.2020.06.021.

9. Li, X., Zhou, R., Zhang, Y.-J. A., Jiao, L., & Li, Z. (2020). Smart vehicular communication via 5G mmWaves. Computer Networks, 172, articl no. 107173.
https://doi.org/10.1016/j.comnet.2020. 107173.

10. Malik, P. K., & Singh, M. (2019). Multiple bandwidth design of micro strip antenna for future wireless communication. The International Journal of Recent Technology and Engineering, 8(2). https://doi. Org/10.35940/ijrte.b2871.078219.

11. Malik, P. K., Wadhwa, D. S., & Khinda, J. S. (2020). A survey of device to device and cooperative communication for the future cellular networks. International Journal of Wireless Information Networks, 27(3), 411–432.
https://doi.org/10.1007/s10776-020-00482-8.

12. Malik, P.K., Wadhwa, D.S. &Khinda, J.S. A Survey of Device to Device and Cooperative Communication for the Future Cellular Networks. Int J Wireless Inf Networks (2020).
https://doi.org/10.1007/s10776-020-00482-8

13. P. Zhang, X. Kang, X. Li, Y. Liu, D. Wu and R. Wang, "Overlapping Community Deep Exploring-Based Relay Selection Method Toward Multi-Hop D2D Communication," in IEEE Wireless Communications Letters, vol. 8, no. 5, pp. 1357-1360, Oct. 2019.

14. A. Liu, L. Lian, V. Lau, G. Liu and M. Zhao, "Cloud-Assisted Cooperative Localization for Vehicle Platoons: A Turbo Approach," in IEEE Transactions on Signal Processing, vol. 68, pp. 605-620, 2020.

15. H. Khelifi et al., "Named Data Networking in Vehicular Ad Hoc Networks: State-of-the-Art and Challenges," in IEEE Communications Surveys & Tutorials, vol. 22, no. 1, pp. 320- 351, First quarter 2020.

16. Liu, N.; Liang, Y.; Zhu, L.; Zhou, H.; Fu, G. A low-profile dual-band shorted patch antenna with enhanced-
bandwidth and multifunctional beams under reshaped modes. Int. J. RF Microw. Comput. Eng. 2021, 31, e22726.

17. Sharma, N.; Bhatia, S.S. Comparative analysis of hybrid fractal antennas: A review. Int. J. RF Microw. Comput. Eng. 2021, 31, e22762.

18. Malallah, R.; Shaaban, R.M.; Al-Tumah, W.A.G. A dual band star-shaped fractal slot antenna: Design and measurement. AEU-Int. J. Electron. Commun. 2020, 127, 153473.

19. Daniel, R.S. A CPW-fed rectangular nested loop antenna for penta band wireless applications. AEU-Int. J. Electron. Commun. 2021, 139, 153891.

20. Patanvariya, D.G.; Chatterjee, A.; Kola, K.; Naik, S. Design of a linear array of fractal antennas with high directivity and low cross-polarization for dedicated short range communication application. Int. J. RF Microw. Comput. Eng. 2020.

21. Kola, K.S.; Chatterjee, A.; Patanvariya, D. Design of a compact high gain printed octagonal array of spiral-based fractal antennas for DBS application. Int. J. Microw. Wirel. Technol. 2020, 12, 769–781.

22. Khalaf, O.I.; Sokiyna, M.; Alotaibi, Y.; Alsufyani, A.; Alghamdi, S. Web Attack Detection Using the Input Validation Method: DPDA Theory. Comput. Mater. Contin. 2021, 68, 3167–3184.

23. Salah H, Robert J, Ahmed H A, et al. Theoretical Performance Evaluation of UHF-RFID Systems with Multi- Antenna Maximum-Likelihood Decoding [J]. IEEE Journal of Radio Frequency Identification, 2019, 3(2): 108-117.

24. Deng W, Li Z, Xia Y L, et al. A Widely Linear MMSE Anti- Collision Method for MultiAntenna RFID Readers [J]. IEEE Communications Letters, 2019, 23(4): 644-647.

25. Shaik, N., & Malik, P. K. (2020). A retrospection of channel estimation techniques for 5G wireless communications. International Journal of Advanced Science and Technology, 29(5), 8469–8479.

26. Rogalski, M. (2021). Security assessment of suppliers of telecommunications infrastructure for the provision of services in 5G technology. Computer Law & Security Review, 41, article no. 105556. https://doi.org/10.1016/j.clsr.2021.